Chemistry and Materials

The Center for Science Innovation

Research Article

Chem. Mater. 2 (2) 2023, 51-55

Scan rate Dependent Factor for Antioxidant Activity of Gold Nanofilms Synthesized via Cyclic Voltammetry Technique

Babay Asih Suliasih[1]*, Dwi Giwang Kurniawan[2], Annisa Auliya[2], Marissa Angelina[3]

[1]Faculty of Pharmacy, Universitas Indonesia, Gedung A Rumpun Ilmu Kesehatan, Kampus UI Depok, Kota Depok, Jawa Barat, 16424, Indonesia

[2]Department of Chemistry, Faculty of Mathematics and Natural Science, Universitas Negeri Jakarta, Jl. Rawamangun Muka, Jakarta 13220, Indonesia

[3]Research Centre for Pharmaceutical Ingredients and Traditional Medicine, National Research and Innovation Agency (BRIN), Kawasan PUSPIPTEK Serpong, Tangerang Selatan Banten 15314, Indonesia

*Corresponding author: babay_asih@farmasi.ui.ac.id

Received
14 June 2023

Received in revised form
21 June 2023

Accepted
26 July 2023

Published online
29 July 2023

DOI
https://doi.org/10.56425/cma.v2i2.60

Abstract

Gold nanoparticles (AuNPs) were found to act as antioxidants owing to their inert, high stability, biocompatibility, and non-cytotoxic. The present investigation involved the synthesis of gold nanoparticles through the electrodeposition technique on a substrate comprising Fluorine-doped Tin Oxide (FTO). By manipulating the scan rate parameter, an effective approach can be employed to facilitate precise management of particle morphology and size. The obtained shape of AuNPs were spherical and irregular. In this study, it was observed that gold nanoparticles elicited potent inhibition, particularly at a scan rate of 150 mV/s, with a markedly high inhibition value of 41.27%. The outcome was further supported by the increase of particles distribution density per unit area, which measured as 149,635,036.5/mm².

Keywords: gold nanoparticle, antioxidant, scan rate, electrodeposition

1. Introduction

Degenerative diseases have emerged as the biggest contributor to mortality rates worldwide. According to the World Health Organization, approximately 17 million died from the disease. Biochemists commenced investigating and elucidating the cause of oxidative metabolic dysfunctions in human beings via the utilization of quantitative calculations. The root cause of the aforementioned phenomenon stems from an overabundance of free radicals within cellular tissue, which causing premature aging, cellular impairment, and the incurable disease [1]. These free radicals that may cause oxidative stress in cellular metabolism are commonly called reactive oxygen species (ROS) [2].

An antioxidant substance is conceptually defined as a compound that has the ability to either directly scavenge reactive oxygen species (ROS) or indirectly modulate the expression of antioxidant defence mechanisms in order to suppress ROS production [3]. Commonly, antioxidant is derived from nature or synthetic. However, several drawbacks have been noted from these antioxidants among others inadequate antioxidant efficiency, unfavourable flavour or odour, potential degradation during the processing stage, susceptibility to radio sensitization, high toxicity especially for synthetic antioxidant and low aqueous solubility [4].

Currently, there is a promising alternative antioxidant known as gold nanoparticle (AuNPs). Numerous studies have reported AuNPs possess antioxidant qualities, which effectively mitigate the detrimental effects of oxidative stress that contributes to the formation of ROS [5–8]. These nanoparticles exhibit inertness, robust stability, biocompatibility, as well as non-cytotoxic properties [9].

A variety of physical, chemical, and biological methodologies are employed for synthesizing AuNPs. Each of these methods exhibits its own limitations, which

include high costs, potentially harmful effects, demanding labor requirements, and various other factors [10]. In this research, we propose an electrodeposition method for synthesizing AuNPs in the form of nanofilm (AuNFs). The utilization of this approach presents various advantages, including but not limited to high purity, reduced cost, accelerated processing, higher deposition rates, ability to overcome shape-related constraints, as well as elimination of the need for after-deposition treatments [11]. Several parameters can be applied in this technique to modify the size and shape of AuNPs. The size and shape of the gold nanoparticles determine their optical, physical, and chemical properties. Moreover, this morphology has the potential to exert significant impacts on various phenomena, such as the enhancement of Raman scattering at surfaces (also known as Surface-enhanced Raman scattering or SERS) and the resonance of plasmons at interfaces (referred to as surface plasmon resonance) [12]. Therefore, this research will investigate the effect of scan rate parameters to the morphology of AuNFs which further contribute to its antioxidant capacity.

2. Materials and Method

A set of materials were employed which included $HAuCl_4$. $3H_2O$ (Sigma-Aldrich), H_2SO_4 (Merck), C_2H_5OH (Merck), NaOH (Merck), KCl (Merck), 2,2-diphenyl-1-picrylhydrazyl (Merck), and distilled water. In addition, a fluorine-doped tin oxide glass (FTO) as a substrate was procured from NSG Pilkington.

The synthesis was performed using 15 mL of 0.5 mM $HAuCl_4.3H_2O$ in 0.5 M H_2SO_4 as the supporting electrolyte, employing cyclic voltammetry technique at a scan rate of 100 mV/s. Subsequently, several scan rates were set within the optimum potential range generated under the previous conditions which was -0.5 V – 0.75 V. The variations in scan rates were as follows: 50 mV/s, 100 mV/s, 150 mV/s, 250 mV/s, and 300 mV/s. AuNPs were synthesized on an FTO substrate that functioned as a working electrode, while platinum was used as the counter electrode, and Ag/AgCl as the reference electrode. All treatments were carried out at room temperature of 25 ˚C. After the electrodeposition process was completed, the substrate was removed from the cell, rinsed with deionized water, and dried again.

The obtained AuNFs were then characterized by energy dispersive X-ray spectroscopy (EDX, Oxford Instrument Xplore 15) and Scanning Electron Microscopy (SEM, Thermoscientific Quanta 650) to investigate its elemental composition and morphology, respectively. The particle size was subsequently determined by ImageJ Software.

The 2,2-diphenyl-1-picrylhydrazyl (DPPH) in vitro test method was used to evaluate the antioxidant activity of AuNFs which examined by microplate reader spectrophotometry (Thermo Scientific™ Multiskan™ GO Microplate). AuNFs with 3 mm x 4.25 mm in size were placed in a 24-well plate and filled with 0.75 ml of a 250 µM DPPH solution dissolved in ethanol. Subsequently, the samples were incubated in the spectrophotometry equipment for various time intervals of 30, 45, 60, 75, and 90 minutes. Prior to measurement, the samples were agitated by shaking. The percent inhibition of DPPH was determined using the similarfollowing equation (1).

$$\% \text{ Inhibition of DPPH} = [(C–S/C)] \times 100\ \% \quad \text{----------} \quad (1)$$

Where, C is absorbance of the DPPH control and S is absorbance of DPPH-AuNFs solution at 516 nm.

3. Results and Discussion

3.1. Characterization of AuNFs

The EDX spectrum confirms the formation of AuNFs on the surface of FTO. In Fig. 1, the spectrum shows signals of Au at 2.2 and 9.8 keV. In addition to Au, there are also spectra of other elements originating from FTO glass, namely Sn and Si.

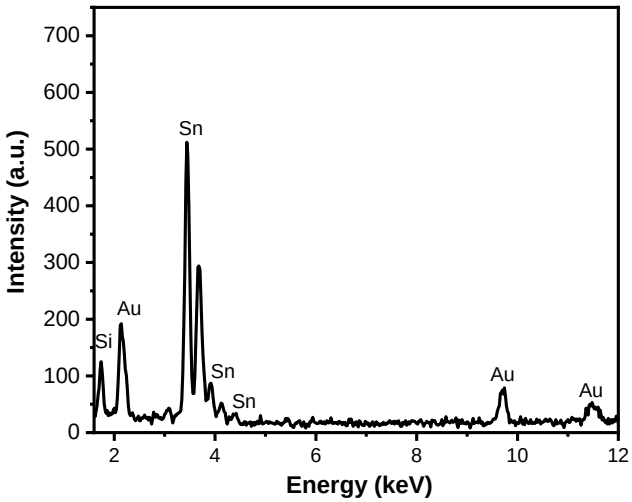

Figure 1. EDX Spectra of AuNFs

The results of the SEM analysis of AuNFs deposited at various scan rates and histogram of particle distribution per unit area are shown in Fig. 2. This SEM analysis revealed that gold nanoparticles, which were deposited at a scan rate of 50 mV/s, manifest a particle density per unit area of 66,909,975. 67/mm² and tend to exhibit a spherical morphology with a diverse range of sizes, as depicted in Fig. 2a. Upon an elevation in scan rate up to 100 mV/s, the shape of the particle becomes irregular form and tends to

have a similar size with a particle distribution per unit area of 98,053,527.98/mm² (Fig. 2b). The morphology of the particles exhibits a predominantly spherical shape, with minor incidences of irregular shaped particles in smaller sizes. However, the enhancement in scan rate to 150 mV/s results in a notably homogeneous distribution of the particles and particle distribution per unit area of 149,635,036. 5/mm, as depicted in Fig. 2c. When subjected to scan rates of 250 mV/s and 300 mV/s, the particles demonstrate comparable circular morphology with small sizes. The results indicate that the number of particles per unit area for 250 mV/s and 300 mV/s is 122,627,737. 2/mm² and 114,111,9221/mm², respectively, as illustrated in Fig. 2d and 2e.

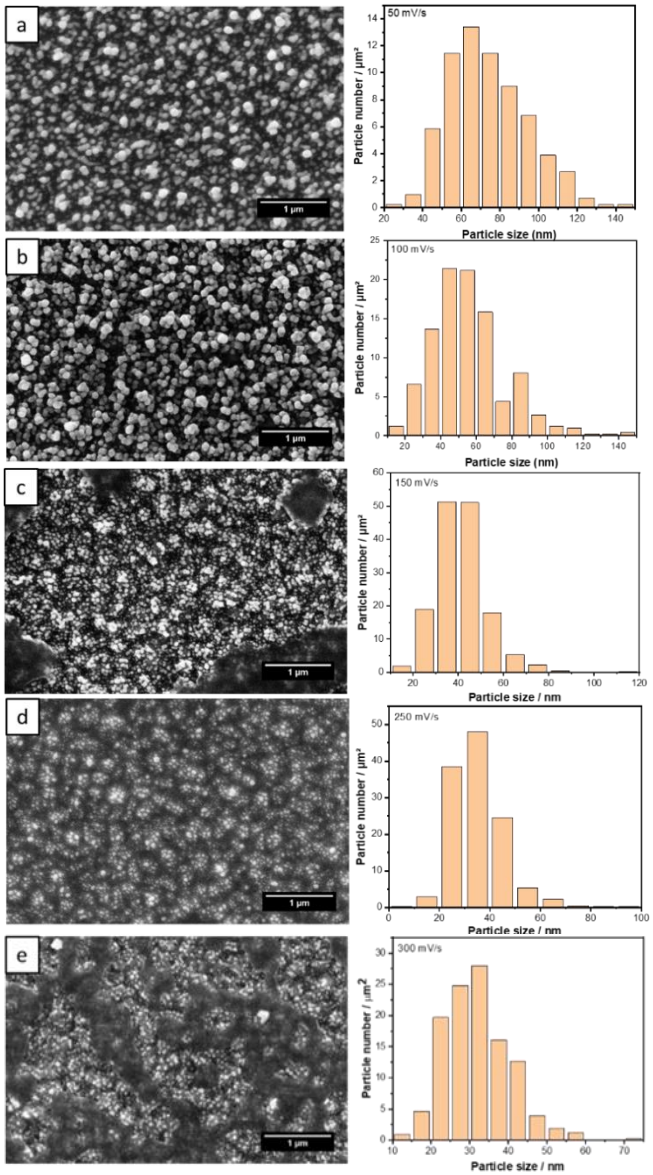

Figure 2. SEM analysis of AuNFs deposited at various scan rates and histogram of particle distribution per unit area.

The phenomenon of particle growth at varying scan rates showed that the increased scan rate triggers a shortened period of deposition process. The acceleration of the particle growth process occurs subsequent to nucleation, leading to non-growth particle and only appear in a spherical shape [13]. In the study conducted by Gao, et.al [14], it was found that extended periods of deposition gave rise to a progression in the morphology of particles from a spherical to an irregular configuration.

3.2. Antioxidant capacity test

All samples showed good response from DPPH in vitro test. Fig. 3 shows a decrease in the absorbance value of DPPH in each sample. This indicates the presence of antioxidant activity, which is further calculated as the % inhibition to identify the most optimal sample.

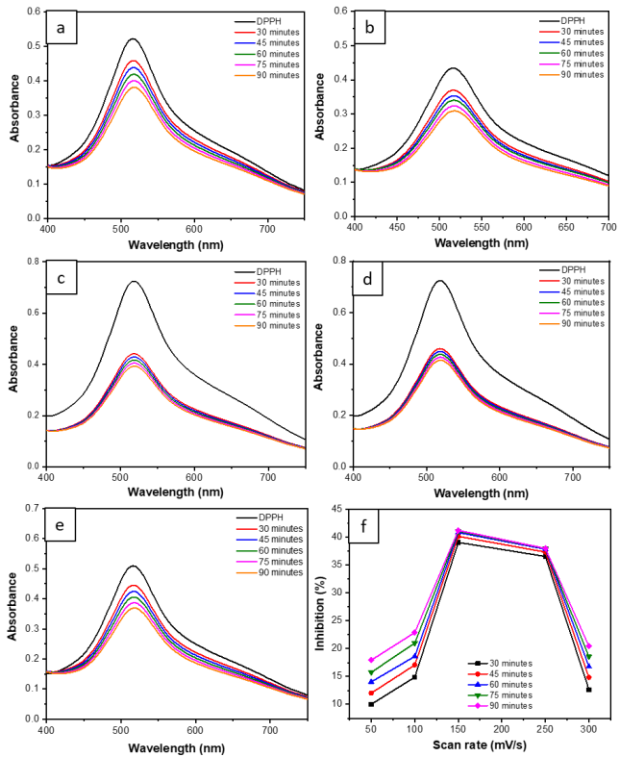

Figure 3. UV–vis spectra of DPPH control and AuNFs samples synthesized at different scan rate (a) 50 mV/s, (b) 100 mV/s, (c) 150 mV/s, (d) 250 mV/s, (e) 300 mV/s, (f) The inhibition percent of AuNFs synthesized at different scan rate.

Based on the graph of inhibition values, the sample at the scan rate of 50 mV/s which has spherical and fewer particles compared to other samples shows an inhibition value of 17.93%. At a scan rate of 100 mV/s, the observed inhibition value was 22.91% with particles exhibited an irregular morphology and were reasonably distributed throughout the sample. At a scan rate of 150 mV/s,

particles with an irregular shape possess a percentage value of 41.27%. This particular specimen demonstrates the most homogenous dispersion and exhibits the greatest number of particles when compared to other samples. At a scan rate of 250 mV/s, the particles showed a more spherical morphology and a tendency to disperse in a group formation with a corresponding inhibition value of 38.03%. At a scan rate of 300 mV/s, the sample also showed spherical particle morphology with an inhibition efficacy of 20.45%. This specific sample exhibits a lower incidence compared to the remaining particles.

The sample that underwent treatment with a scan rate of 150 mV/s and possessed the highest number of particles exhibited the greatest degree of inhibition, as indicated by the highest percentage of inhibition observed. The number of particle value is positively correlated with the concentration of gold nanoparticles, whereby an increase in the number of particles results in a corresponding increase in concentration that contribute to increase of antioxidant capacity [15].

4. Conclusion

Gold nanofilms were successfully synthesized using the electrodeposition method with variations of the scan rate. The findings from the SEM analysis demonstrated that the fabricated gold nanoparticles possess heterogeneous particle distributions and present with structurally irregular and spherical morphologies. According to the in vitro DPPH assay result, it can be inferred that the sample treated with a scan rate of 150 mV/s displayed the greatest antioxidant capacity, attaining an impressive value of 41.27%. The assertion was corroborated through analysis of the collected data, whereby it was revealed that the studied sample exhibited the most substantial particle number of 149,635,036.5 particles/mm².

Acknowledgment

This research was supported by LPPM Universitas Negeri Jakarta through the research scheme Penelitian Kolaboratif International with contract number 9/KI/LPPM/IV/2021.

References

[1] E.I. Korotkova, Y.A. Karbainov, A. V. Shevchuk, Study of antioxidant properties by voltammetry, *J. Electroanal. Chem.* **518** (2002) 56–60. https://doi.org/10.1016/S0022-0728(01)00664-7.

[2] V.I. Lushchak, Free radicals, reactive oxygen species, oxidative stress and its classification, Chem. Biol. Interact. **224** (2014) 164–1. https://doi.org/10.1016/j.cbi.2014.10.016.

[3] İ. Gulcin, Antioxidants and antioxidant methods: an updated overview, (2020). https://doi.org/10.1007/s00204-020-02689-3.

[4] C.J. Mbah, I. Orabueze, N.H. Okorie, Antioxidants Properties of Natural and Synthetic Chemical Compounds : Therapeutic Effects on Biological System, *Acta Sci. Pharm.* Sci. **3** (2019) 28–42. https://doi.org/10.31080/ASPS.2019.03.0273.

[5] J. Djajadisastra, Sutriyo, P. Purnamasari, A. Pujiyanto, Antioxidant activity of gold nanoparticles using gum arabic as a stabilizing agent, *Int. J. Pharm. Pharm*. Sci. **6** (2014) 462–465. https://doi.org/10.31080/ASPS.2019.03.0273.

[6] H. AI, E.B. AF, R. M., Antitumor and Antioxidant Activity of Gold Nanoparticles: In vitro and In vivo Study, *Sci. J. Oct. 6 Univ*. **3** (2016) 28–34. https://doi.org/10.21608/sjou.2016.31738.

[7] G. Balasubramani, R. Ramkumar, R.K. Raja, D. Aiswarya, C. Rajthilak, P. Perumal, Albizia amara Roxb. Mediated Gold Nanoparticles and Evaluation of Their Antioxidant, Antibacterial and Cytotoxic Properties, *J. Clust. Sci.* **28** (2017) 259–275. https://doi.org/10.1007/s10876-016-1085-9.

[8] S. Naraginti, Y. Li, Preliminary investigation of catalytic, antioxidant, anticancer and bactericidal activity of green synthesized silver and gold nanoparticles using Actinidia deliciosa, J. Photochem. *Photobiol. B Biol.* **170** (2017) 225–234. https://doi.org/10.1016/j.jphotobiol.2017.03.023.

[9] A. Lohani, A. Verma, H. Joshi, N. Yadav, N. Karki, Nanotechnology-Based Cosmeceuticals, ISRN Dermatol. **2014** (2014). https://doi.org/10.1155/2014/843687.

[10] S. Thota, D. C.Crans, Metal Nanoparticles: Synthesis and Applications in Pharmaceutical Sciences, *wiley-VCH Verlag GmbH & Co*, (2018). https://doi.org/10.1002/9783527807093.

[11] I. Gurrappa, L. Binder, Electrodeposition of nanostructured coatings and their characterization : a review, **9** (2008). https://doi.org/10.1088/14686996/9/4/043001.

[12] E.C. Dreaden, A.M. Alkilany, X. Huang, C.J. Murphy, M.A. El-Sayed, The golden age: Gold nanoparticles for biomedicine, *Chem. Soc. Rev.* **41** (2012) 2740–2779. https://doi.org/10.1039/c1cs15237h.

[13] M. Etesami, F.S. Karoonian, N. Mohamed, Electrochemical deposition of gold nanoparticles on pencil graphite by fast scan cyclic voltammetry, J. Chinese Chem. Soc. 58 (2011) 688–693. https://doi.org/10.1002/jccs.201190107.

[14] F. Gao, M.S. El-Deab, T. Okajima, T. Ohsaka, Electrochemical Preparation of a Au Crystal with

Peculiar Morphology and Unique Growth Orientation and Its Catalysis for Oxygen Reduction, *J. Electrochem. Soc.* **152 (**2005) A1226. https://doi.org/10.1149/1.1906023.

[15] J. Shang, X. Gao, Nanoparticle counting: Towards accurate determination of the molar concentration, *Chem. Soc. Rev*. **43** (2014) 7267–7278. https://doi.org/10.1039/c4cs00128a.